Vacuum 83 (2009) 1200–1203

Contents lists available at ScienceDirect

Vacuum

journal homepage: www.elsevier.com/locate/vacuum

Ag/PEO nanocomposite fabricated in a planar magnetron sputtering

Lei Yue [a,c], Meili Zhou [a], Qiang Chen [a,*], Jing Weng [b], Yuefei Zhang [a]

[a] Laboratory of Plasma Physics and Materials, Beijing Institute of Graphic Communication, Xinghua North Street 25, Daxing, Beijing 102600, China
[b] Capital Medical University, Beijing 100069, China
[c] Shandong Publishing Polytechnic College, 250022, China

ARTICLE INFO

Article history:
Received 26 August 2008
Received in revised form
10 October 2008
Accepted 19 October 2008

Keywords:
Magnetron sputtering
Ag/PEO
Nanocomposite

ABSTRACT

Thin films of silver (Ag)/polyethylene-oxide (PEO) nanocomposite were fabricated by a co-deposition of Ag sputtering particles and PEO thin film on substrates using a planar magnetron sputtering system. The PEO were polymerized from the monomer ethyl glycol dimethyl ether in the magnetron sputtering (MS) plasma. The nanocomposites were characterized by using UV-visible spectroscopy, X-ray photoelectron spectroscopy (XPS), X-ray diffraction (XRD) and atomic force microscopy (AFM). The correlation was performed between the concentrations of Ag and functional group density in Ag/PEO nanocomposites with the discharge parameters, such as sputtering gas pressure and the distance of target-to-substrate. By using AFM and XRD, it is illustrated that the Ag particles distribute uniformly in the body of nanocomposite and remain in atomic status with preferential growth in facet of (111).

© 2008 Published by Elsevier Ltd.

1. Introduction

Recently, there is increasing interest in plasma-deposited thin films that possess bacteria-resistant and non-fouling properties, especially in biological medicine where medical device infection is associated with significant healthcare costs [1,2]. Different approaches for preventing microbial adhesion or for inhibiting bacterial growth have been proposed [3]. The organic polymer polyethylene oxide (PEO) is one of the most well-known [4,5] biomaterials for non-fouling behaviors in cells' bacteria, and proteins are especially emphasized at present. Silver (Ag), on the other hand, is one of the classical antibacterial reagents. Through the permeation of Ag ion onto the cell wall, it is considered that Ag can suppress bacterial enzyme activity and inhibit the cell proliferation by binding to DNA chains [6,7]. The nanocomposite of Ag/PEO is one of the most promising candidates as a bacteria-resistant coating and anti-infective application for biomedical devices because it merges the non-fouling properties of PEO [4,5,8] and the antimicrobial properties of Ag [9,10].

For PEO to obtain non-fouling characteristics by the plasma polymerization process, it is indispensable that the structure of the functional group C–C–O in monomer shall be retained as much as possible in the PEO coating, whereby the plasma polymerization conditions should comprise fragmentizing the monomer and polymerizing the functional group film in a mild input power. For a metal film deposition such as by means of a magnetron sputtering (MS) process, however, the conditions are quite different, in that high energetic ions are needed to impact the target and generate a dense species flux. Therefore, for the fabrication of nanocomposite Ag (metal)/PEO (organic), a novel method shall thus be proposed in order to polymerize a proper density of functional group on the surface and deposit a critical concentration of Ag for antimicrobial properties at the same time.

In this paper we present a strategic purpose on nanocomposite Ag/PEO deposition, where the nanocomposites were fabricated in a planar magnetron sputtering plasma.

2. Experimental section

Ag/PEO films were prepared by direct current supply (DC) MS. The sputtering target consists of 99.99% Ag in diameter of 50 mm, and the PEO was polymerized from monomer ethyl glycol dimethyl ether (EGDME) vapor. A metal vacuum chamber of a sputtering apparatus was preliminarily evacuated to 3×10^{-3} Pa.

During Ag/PEO composite film deposition the total pressure was varied from 0.2 to 2.0 Pa, which was realized by the change of the pump speed, the distance of target-to-substrate was varied from 60 mm to 100 mm, and the total flow rate (Ar flow rate was 10 sccm for Ag sputtering, and monomer flow rate was 2 sccm for PEO polymerization), and DC input power (20 W) were kept constant. Substrates were put on a water-cooled magnetron cathode assembly, keeping the temperature used for sample preparation at ambient temperature. Typical film thicknesses were in the range of 30–60 nm.

* Corresponding author. Tel.: +86 10 6026 1099; fax: +86 10 6026 1108.
E-mail address: chenqiang@bigc.edu.cn (Q. Chen).

0042-207X/$ – see front matter © 2008 Published by Elsevier Ltd.
doi:10.1016/j.vacuum.2008.10.006

www.cpm.com.cn

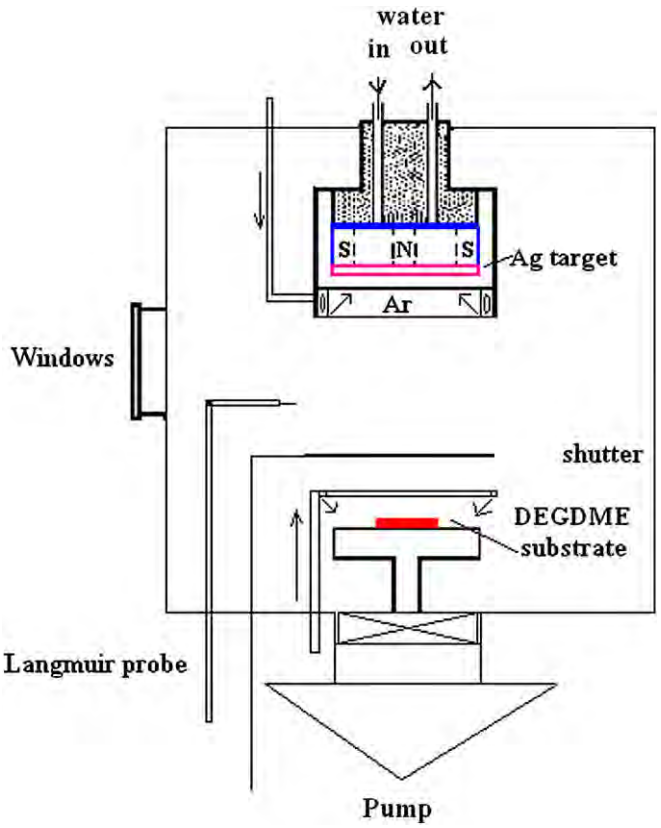

Fig. 1. The schematic diagram of the deposition system.

Fig. 1 shows the schematic deposition system of the present experiments and Table 1 is the typical deposition parameters. The monomer EGDME vapor controlled by mass flow controllers was introduced just above the substrate, and Ar (99.99%) fed at 10 sccm into the chamber through mass flow controllers was near the target surface. A shutter used to protect the substrate was moved after Ag target was pre-sputtered for 5 min and the monomer flowing was stable.

The silicon wafers and quartz slides as substrates were cleaned sequentially in an ultrasonic bath using ethanol, acetone, and de-ionized water before they were mounted on the sample holder. The thickness of Ag/PEO films was measured by a profilometer (AMBISOS, XP-2). The chemical structures were determined by X-ray photoelectron spectroscopy (XPS, Kratos Axis ULTRA, using a monochromatic Al $K\alpha$ source and a charge neutralizer). Atomic force microscopy (CSPM 3000, Ben Yuan, China) operating in a tapping mode was used to investigate surface morphology. The Ag crystal facets were investigated by X-ray diffraction (XRD, Rigaku D/max-2400 with Cu $K\alpha$, radiation $\lambda = 0.154056$ nm).

3. Results and discussion

3.1. XRD analysis

The present composite films comprising Ag crystallites are revealed by XRD pattern in Fig. 2, where the detail of Ag crystalline

Table 1
The typical deposition parameters in this experiment

Distance of target-to-substrate (mm)	Working pressure (Pa)	Power (W)	Ar flow rate (sccm)
90 mm	0.2	20	10
80 mm	0.5		
70 mm	1.0		
60 mm	2.0		

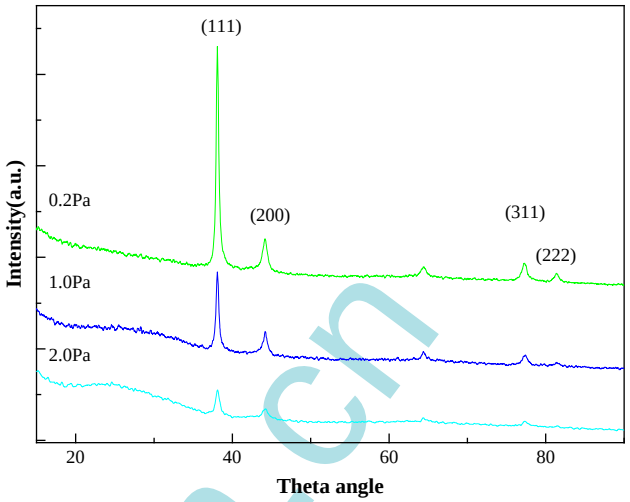

Fig. 2. XRD pattern of Ag/PEO composite film dependent on the working pressure.

absorption peaks is tracked in XRD pattern as a function of the sputtering gas pressure, and the Ag/PEO coatings were deposited onto a quartz slide surface. The Ag crystalline corresponding to (111), (200), (311) and (222) are clearly observed in this figure. It is observed that the intensity in patterns increases with the sputtering gas pressure decreasing from 2.0 Pa to 0.2 Pa. This means that the growth rate was rapid in low pressure and the concentration of Ag in the matrix was high in this condition. Moreover, the relative peak intensity of the (111) facet is significantly high in pattern in 0.2 Pa implies that the Ag crystalline has preferential growth in facet of (111) at low pressure. The strong crystal orientation of Ag particles at the low sputtering gas pressure displays that the crystal status of Ag in the present composite film can be tunable by the variation of the discharge conditions such as the sputtering gas pressure in convenience. Such results are very important for the application of Ag/PEO(-like) composite in antimicrobial films, where the diameter and (111) facet orientation of Ag crystalline play a dominant role in denaturing the bacteria [15].

3.2. Chemical structures of Ag/PEO and PEO films by XPS

Fig. 3 shows typical XPS spectra of the films which were co-deposited by Ag and PEO Fig. 3(a–c)), and the pure PEO Fig. 3(d). The C1s peak in films was deconvoluted in Gausses model. One is noted that the coatings contain three separated peaks, namely C_0 (C–H, C–C: BE = 285.0 eV), C_1 (C–OH, C–O–C; BE = 286.5 eV), and C_2 (O–C–O, C–O; BE = 287.8 ± 0.2 eV). Assuming that the C_1 peak is only due to carbon atoms in C–O–C moieties, thus the percent area of C_1 with respect to the total C1s peak can be taken as a measurement of the EO concentration in PEO coatings. Then the approximation of C–C–O (EO) concentration can be performed since the contribution of C–OH groups on the peak is usually assumed very low for plasma-deposited PEO [5,8,11–13].

From Fig. 3 one finds that the contents of Ag and EO in composites remarkably depended on the distance of target-to-substrate, but no unambiguous relationship. The contents of both Ag and EO were maximized when the distance was at 90 mm. It is in agreement with the FTIR spectra of Ag/PEO coatings which also display the C–C–O peak is strongest when it was polymerized in this distance.

It is also found that the influence of distance of target-to-substrate on the concentration of Ag and EO is quite different. In 75 mm the concentration of EO was 17.5%, and Ag was 0.7%; when the distance increased to 100 mm the EO concentration was 21%

www.spm.com.cn

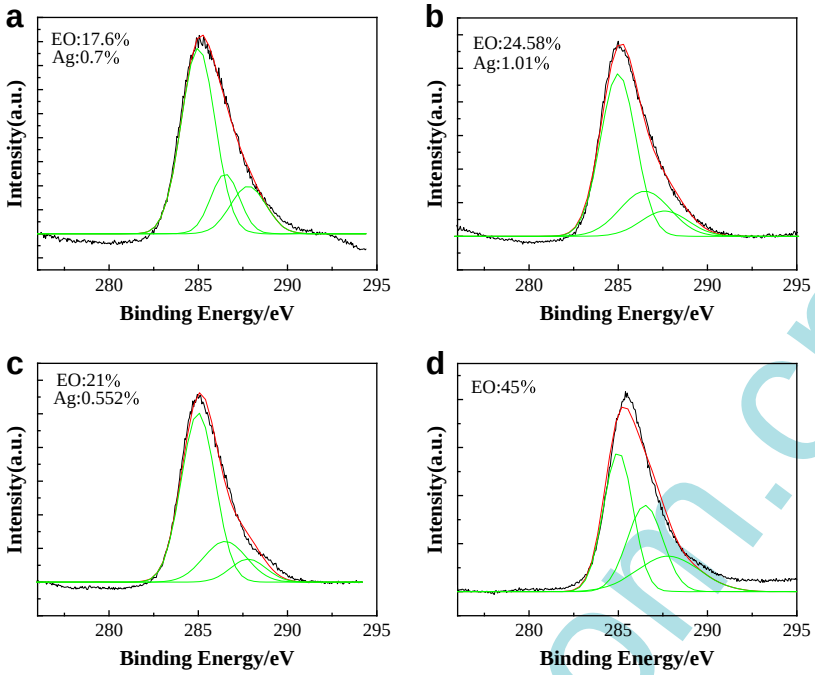

Fig. 3. Relative density trend of C and O in Ag/PEO composite detected by means of X-ray photoelectron spectroscopy (XPS) in different distances of target-substrate ((a) 75 mm; (b) 90 mm; (c) 100 mm; d- 75 mm, only PEO polymerization. The ether component of the C1s absorption peak is at about 286.5 eV).

and Ag was 0.552%, where EO concentration was increased and Ag concentration was decreased in contrast; when the distance was at 90 mm, the concentration became 24.58% and 1.01%, respectively.

Compare Fig. 3(a)with (d), which was in identical condition, one obtains that the EO content is greatly decreased in sputtered Ag co-deposition with PEO processing, where EO is 17.6% instance of 45% in pure PEO polymerization processing.

Through a profilometer (AMBISOS, XP-2), the relationship of deposition rate with the distance of target-to-substrate was correlated. The thickness of Ag/PEO films decreased along with the distance, and the deposition rates were 13.4 ± 0.5 nm/min, 14.5 ± 0.5 nm/min, 17.8 ± 1 nm/min and 21.5 ± 1 nm/min corresponding to the distance of 90 mm, 80 mm,70 mm and 60 mm, respectively.

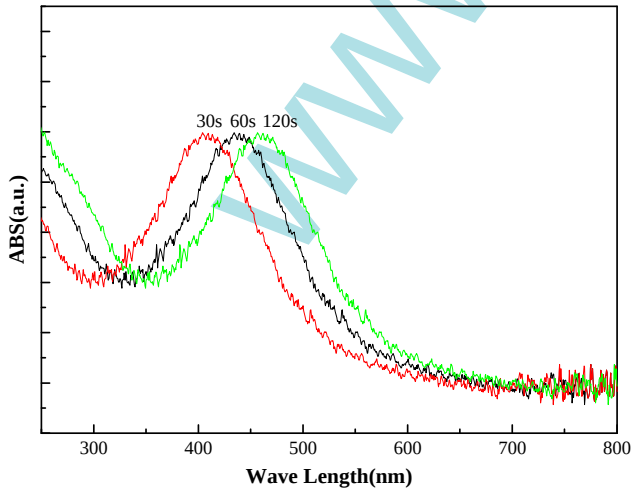

Fig. 4. Detail of surface plasmon resonance peak of Ag particles tracked in the UV-visible spectra as a function of the deposition time (the Ag/PEO coatings were deposited onto quartz samples).

Fig. 4 shows the UV-visible spectra of the Ag/PEO nanocomposites in the range of 300–800 nm. In the UV-visible spectra, the absorption peak induced from the surface plasmon transverse resonance of Ag particle is obviously illustrated. The peak located at ca. 400 nm in spectra demonstrates that Ag particle is in atomic status. Increasing the deposition time leads to a red-shift of the main peak (from 410 nm to 460 nm when exposure time was extended from 30 s to 120 s). The red-shift of peak location might be attributed to the size increase of metal nanoparticles formed in polymer matrix or the oxidation of the Ag particles [14].

3.3. Morphology

Fig. 5 presents the AFM images of PEO and Ag/PEO films. It can be clearly seen that the PEO film was formed by isolated nanoparticle in island growth model in pure PEO polymerization process. The AFM images of the PEO coatings and the ones embedded with nanoparticle Ag are significantly different. The island in PEO film ranges from 1.3 to 3.0 ± 0.5 nm in diameter with the roughness of root mean square (RMS) 5.6 nm. After the Ag was added in the composite, however, the surface roughness demonstrates itself to be extremely high, and the isolated columns are not only larger in diameter, but are also higher in the volume configuration. It is estimated that the columns ranges from 2.5 to 6.7 ± 0.5 nm in diameter with the roughness of RMS 18.4 nm. It is assumed from morphologies that Ag atoms were aggregated in the matrix during the film deposition and growth processes. The increase in the column diameters means that the Ag nanoparticles can be mobilized and aggregated when they arrive at substrates.

4. Conclusions

In this work, Ag/PEO nanocomposites were fabricated in MS plasma, where the Ag nanoparticle was sputtered from target and the organic PEO polymer was polymerized simultaneously from liquid monomer in only a one-dry step process. By XPS it reveals that compounds of PEO and Ag depended on the distance of

www.xjom.com.cn

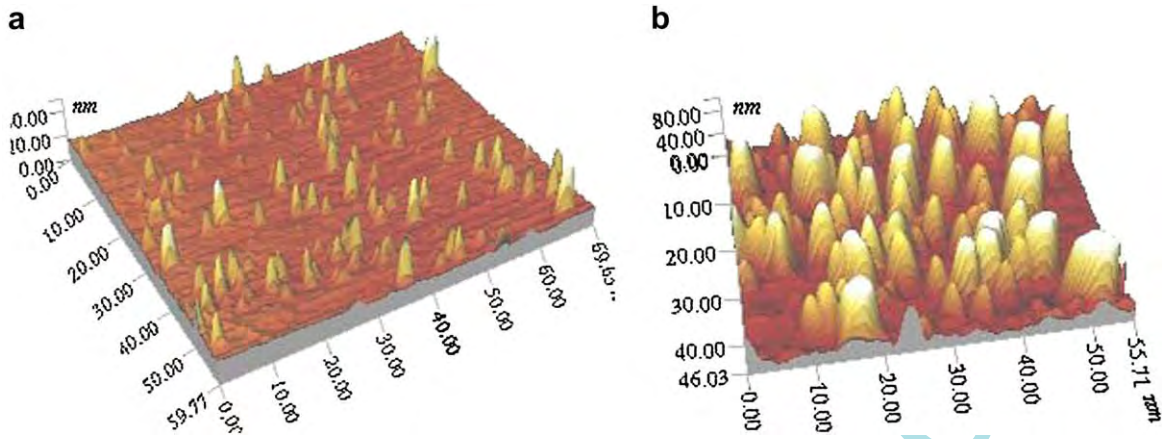

Fig. 5. AFM photos of PEO non-fouling coating (a) and Ag/PEO nanocomposite film (b) on silicon wafers.

target-to-substrate. When the distance of target-to-substrate was at 90 mm the EO concentration could reach 24.58%. AFM and XRD reveal that Ag nanoparticles were uniformly embedded in composite and oriented preferentially in (111) facet. According to our results, one can conclude that Ag concentration, the orientation of Ag nanocrystalline and EO group contents can be tunable by the variation of discharge conditions. In particular the Ag crystal preferential growth facet of (111), which plays the dominant role in Ag nanoparticle antibacterial behavior, can be obtained by deposition in low working pressure. From this experiment we provide a novel strategic method, that MS can be used to generate a non-fouling and antibacterial nanocomposite.

Acknowledgements

This work is supported by NSFC (No.1775017, 10475010), the Beijing Key Scientific Research Foundation for Returned overseas, and PHR (IHLB), KF 060201. The authors also gratefully thank Ms. Kline Kim for her kindness help to review this manuscript.

References

[1] Naylor PT. Clin Orthop Relat Res 1990;261:126–33.
[2] Lin TL, Lu FM, Sheu MS. Med Device Technol 2001;1(8):26–30.
[3] Furno F, Morley KS, Wong B, Sharp BL, Arnold PL, Howdle SM, et al. J Antimicrob Chemother 2004;54:1019–24.
[4] Prime KL, Whitesides GMJ. Am Chem Soc 1993;115:10714–21.
[5] Johnston EE, Ratner BD, Bryers JD. In: d'Agostino R, Favia P, Fracassi F, editors. Plasma-processing of polymers. NATO ASI Series, E: Appl. Sci. Kluwer Academic Publisher; 1997. p. 123–45.
[6] Thurman RB, Gerba CP. CRC Crit Rev Environ Contr 1989;18:295–315.
[7] Bragg PD, Rainnie DJ. Can J Microbiol 1974;20:883–9.
[8] Lopez GP, Ratner BD, Tidwell CD, Haycox CL, Rapoza RJ, Horbett TA. J Biomed Mater Res 1992;26:415–39.
[9] Oloffs A, Grosse-Siestrup C, Bisson S, Rinck M, Rudolph R, Gross U. Biomaterials 1994;15:753–8.
[10] Schierholz JM, Lucas LJ, Rump A, Pulverer G. J Hosp Interface 1998;40:257–62.
[11] d'Agostino R. In: d'Agostino R, Favia P, Fracassi F, editors. Plasma processing of polymers. NATO ASI Series E: Appl Science. Kluwer Academic Publisher; 1997. p. 346–59.
[12] Foerch R, Beamson G, Briggs D. Surf Interface Anal 1991;17:842–7.
[13] Everhart DS, Reilley CN. Anal Chem 1981;53:665–76.
[14] Sen S, Mahanty S, Roy S, Heintz O, Bourgeoi S. Thin Solid Films 2005;474:245–9.
[15] Morones JR, Elechiguerra JL. Nanotechnology 2005;16:2346–53.

www.sfm.com